First-principles calculations of helium and neon desorption from cavities in silicon

2012 J. Phys.: Condens. Matter 24 175006

(http://iopscience.iop.org/0953-8984/24/17/175006)

IOP PUBLISHING JOURNAL OF PHYSICS: CONDENSED MATTER

J. Phys.: Condens. Matter **24** (2012) 175006 (8pp) doi:10.1088/0953-8984/24/17/175006

First-principles calculations of helium and neon desorption from cavities in silicon

A Charaf Eddin and L Pizzagalli

Department of Physics and Mechanics of Materials, Institut P', CNRS—Université de Poitiers—ENSMA UPR 3346, SP2MI, BP 30179, F-86962 Futuroscope Chasseneuil Cedex, France

E-mail: Laurent.Pizzagalli@univ-poitiers.fr

Received 15 December 2011, in final form 1 March 2012
Published 5 April 2012
Online at stacks.iop.org/JPhysCM/24/175006

Abstract

Combining density functional theory, the nudged elastic band technique, and the ultradense fluid model, we investigated the desorption process of He and Ne in silicon. Our results show that the internal surfaces of gas-filled bubbles are not a limiting factor during desorption experiments, since the surface reconstruction opens diffusion paths easier than in the bulk. We show that the vibrational contribution to the energy of helium in the bulk has to be considered in order to determine realistic pressures in the bubbles, when comparing experiments and simulations. At the maximum of desorption, an average pressure of 1–2 GPa is computed.

(Some figures may appear in colour only in the online journal)

1. Introduction

Light noble gases like He and Ne are characterized by several common properties, such as the quasi-absence of chemical reactivity. In fact, the completeness of their valence electron shells makes the formation of chemical bonds very unlikely. This specific property explains why they can provide a quasi-inert atmosphere, which is used, for instance, for the growth process of semiconductors. However, despite this extremely low reactivity, they have been shown to be able to induce significant structural modifications when they are introduced into many solid materials. The results appear to be similar in most cases. Depending on the conditions, noble gas atoms tend to agglomerate, ultimately leading to the formation of cavities with disc or spherical shapes. The generally accepted driving force for this defect formation is the fact that noble gas atoms are insoluble in most materials, their heat of solution being positive. The cavities formed can then be at the origin of several evolution mechanisms such as swelling, surface blistering and plane cleavage, which will irreversibly change the material properties. This process can be clearly labelled 'multi-scale', ranging from the formation of gas-filled cavities at the atomic scale to the possible exfoliation of the material at the macroscale.

There have been many studies devoted to the formation of these cavities, the earliest ones being more specifically focused on helium in metals [1–4]. This interest was largely driven by nuclear materials research. In fact, helium production by neutron capture reactions is an important source of helium in the metal containers or reactor fuels in fission-type reactors. Helium generation in plasma fusion devices was another reason for this research. In all cases, the accumulation of helium in structural materials like steel or bcc metals leads to the formation of He-filled cavities. Besides, the metallic character is not an essential feature, since it was shown that a similar process could be observed in covalent systems like silicon. Again, most of the studies have been focused on He [5–7], although works on Ne [8, 9] have been performed too. A light noble gas like He was demonstrated to be potentially useful for the gettering process in the electronics industry [10]. He atoms are initially implanted in the material, far from the active layers of the future device. Subsequent thermal treatments lead to the formation of voids [11], which are then used to trap undesirable impurities, mostly metallic, migrating from active layers.

Annealing He-filled cavities leads to the desorption of He atoms from the materials [1, 5, 12]. In the case of silicon, several thermal desorption spectrometry experiments have been performed, which have shown that desorption occurs through a single mechanism, with an associated activation energy ranging from 1.7 eV [13] to 1.8 eV [6, 7]. The desorption process can be decomposed along three steps: the He atom has to first leave the cavity by crossing the internal

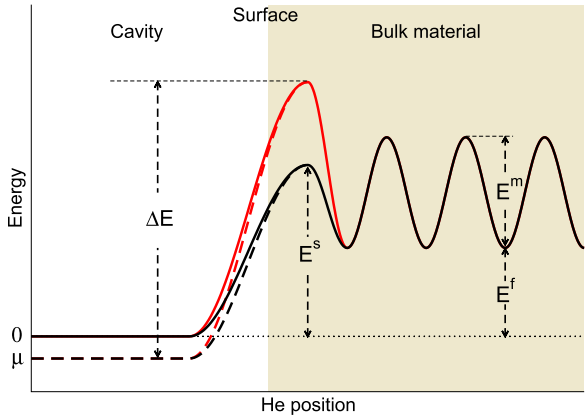

Figure 1. Schematic representation of possible energy variations associated to the desorption of an He atom from a cavity: with a low surface barrier (black), with a high surface barrier (red), and taking into account the free energy of He in the cavity (dashed lines).

surface, then migrates into the material, and finally leaves by crossing the external surface. This simple picture obviously neglects more complex processes which may occur such as retrapping of the He atom by neighbouring cavities. It is similar to a permeation process, especially for large cavities, which may explain the very good agreement of the values above and pioneering permeation experiments [14].

The energy variation for the first two steps is schematically represented in figure 1. It is usually assumed that the energy barrier for the He atom to leave the cavity is lower than the sum of E^{f} and E^{m}, i.e. lower than the sum of the solution and migration energies of He into silicon. Then the desorption energy ΔE is simply $E^{\mathrm{f}} + E^{\mathrm{m}}$. Earlier first-principles calculations of E^{f} and E^{m} have been performed, with sums of 1.59 eV [15] and 2.7 eV [16]. Recent values computed by Charaf Eddin *et al* [17] lead to a sum of 1.87 eV. All of these studies considered that He diffuses as an interstitial in silicon. Nevertheless, it remains to be checked whether the desorption energy can be effectively obtained as the sum of formation and migration energies. In fact, one may wonder about the possible influence of the internal surfaces of the cavity on the desorption process. If the energy barrier E^{s} for crossing the surface is high, as represented in figure 1, the surface could be the limiting factor for desorption. Another important point is the influence of pressure and temperature on the desorption mechanism. Thermal contributions to the energy should be taken into account for point defects in solid materials, and there must be an even larger influence of temperature and pressure on the free energy of helium in cavities, since it is expected to be in a fluid state [18]. We designate as μ the temperature and pressure dependent part of the free energy of an He atom in a cavity (the rest being the internal energy). The desorption energy obviously depends on μ (see figure 1), which should therefore be considered in theoretical studies.

In this work, we investigated the influence on desorption of internal surface crossing, considering the effect of temperature and pressure, for He-filled and Ne-filled cavities in silicon. First-principles calculations in association with the nudged elastic band (NEB) method [19], and numerical simulations using the ultradense fluid model [5], are described in section 2. Our first-principles results are then reported for He and Ne, followed by an analysis of the influence of temperature and pressure in the case of He.

2. Models and methods

Cavities filled with He and Ne obtained by implantation usually exhibit spherical shapes. The diameters of these so-called bubbles range from a few nanometres to few tens of nanometres, depending on the conditions [9, 20–23]. Since these defects are large and a significant region of the surrounding silicon matrix should be included in a simulation, a first-principles calculation seems hardly possible. However it is not necessary to model the entire defect to investigate desorption. As shown in figure 2, our computational system describes a small area of the internal surface of a cavity. In fact, except for the smallest ones, cavities are characterized by well-defined facets with low energies, such as (111) or (001). Here we considered a (001) orientation.

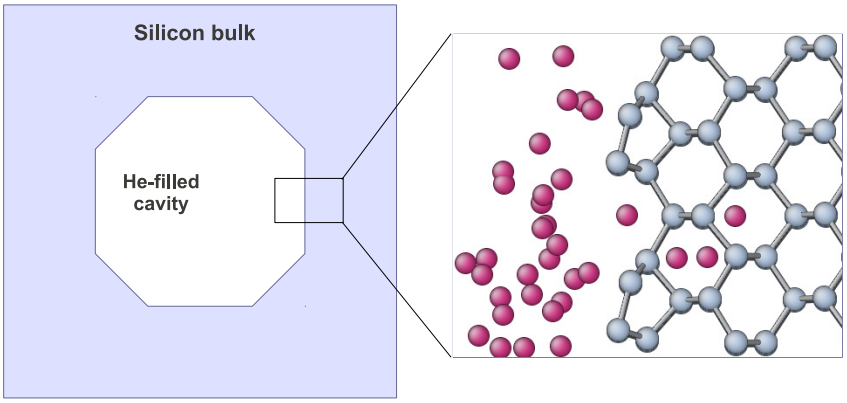

Figure 2. The model used in our calculations. Only a small region of a large facetted cavity (left) is taken into account in our simulations (right).

The model represented in figure 2 includes two well-defined parts, with the silicon matrix in a solid state and the condensate He (or Ne) in a fluid state. Different methods have to be used for each part. First, the silicon matrix in interaction with a single He (or Ne) atom is computed with a first-principles approach in the framework of density functional theory (DFT) [24, 25]. It is modelled by a slab including nine (001) layers of 16 Si atoms each, which is placed in a periodically repeated supercell. Two (001) surfaces are created by introducing a vacuum of 10.94 Å along the [001] direction. The lattice parameter is 5.468 Å, leading to supercell dimensions of 15.468 Å × 15.468 Å × 23.239 Å. A (2 × 1) reconstruction is set on both surfaces, yielding two rows of four surface silicon dimers. One of the surfaces is left bare in order to reproduce the internal cavity surface. The other surface is passivated with hydrogen atoms in order to avoid charge sloshing during electronic structure calculations.

We used the PWscf code in the Quantum-espresso package [26]. Electronic wavefunctions were expanded on a plane waves basis with an energy cutoff of 10 Ryd. For the Brillouin zone sampling, only the Γ point was considered, which was accurate enough since we used a large system. These parameters are slightly below the actual standards of DFT calculations, which is justified by the numerous NEB calculations that we performed. The exchange–correlation contributions were modelled by the PBE generalized gradient approximation [27]. Only valence electrons were considered in our calculations, thanks to the use of the ultrasoft pseudopotentials *Si.pbe-n-van.UPF*, *He_pbe_van.UPF* and *H.pbe-rrkjus.UPF* for Si, He and H from www.quantum-espresso.org. For Ne, we generated an appropriate pseudopotential using the USPP package. Finally, in our calculations the Si atoms belonging to the subsurface layer of the hydrogenated surface were set to ideal bulk positions and were not relaxed in order to mimic the bulk behaviour. For the remaining atoms, simple relaxation and NEB calculations were performed using a relaxation criterion on forces of 10^{-3} eV Å^{-1}.

We checked the validity of our DFT calculations by comparing our results for the relaxed bare Si(001) surface with the literature. We found an asymmetric relaxation of the surface dimers in very good agreement with previous works [28, 29]. It is more difficult to show the validity of our calculations for reproducing the interaction between the silicon and the noble gas. It is known that the PBE functional is not appropriate for describing long-range weak dispersive interactions. Fortunately, here we are interested in noble gas atoms embedded into silicon for which the interaction is essentially repulsive, i.e. short-ranged and large. DFT–PBE should then be appropriate in that case.

For the second part, we need to model the noble gas atoms in a fluid state. Obviously, the simple perfect gas model is not suited for the high pressures that are expected in filled cavities. Here, the ultradense fluid model proposed by Cerofolini *et al* was used [5]. It allows the building of the partition function of a set of confined particles in a fluid state, with a high density. From this partition function, the total free energy as well as the pressure and the chemical potential of one particle can be obtained. The ultradense fluid model is built from a van der Waals model, in which finite-size effects are taken into account by associating a defined constant volume to each particle (the covolume), and by including the interaction energy between all particles. To allow for a better description of the very high particle density, the covolume depends on the particle density and the temperature in the ultradense fluid model. In practice, we used here a Buckingham potential to model the interactions between particles. Only helium was described with this model, using the parameters given in [5].

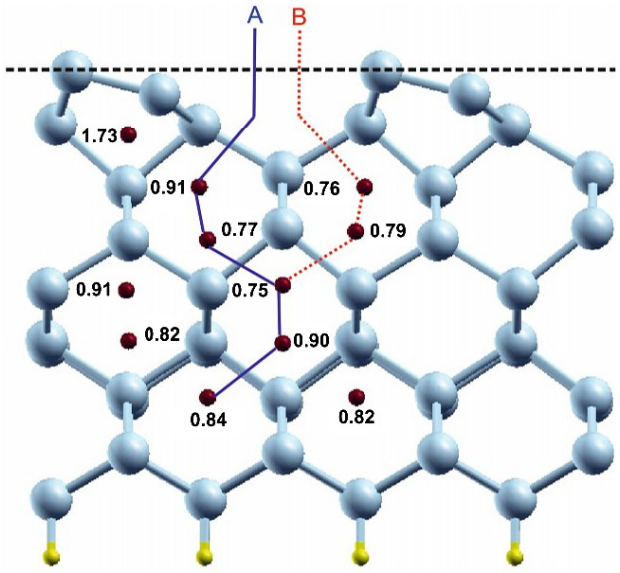

Figure 3. Formation energies in eV of the possible configurations for He in an interstitial position, shown together with the reconstructed Si(001) surface (relaxed with no He). The A and B paths are investigated for He and Ne diffusion from the cavity to the silicon bulk by crossing the surface.

3. He:Si(001) system

All previous studies have shown that the most stable configuration for a single He in bulk silicon is obtained for the tetrahedral interstitial, with formation energies ranging from 0.77 to 1.28 eV [15–17, 30]. In our system, several inequivalent interstitial configurations are possible, due to the presence of the reconstructed surface. All of these were investigated and found to be stable. Figure 3 shows the different computed formation energies. Starting from the surface, it appears that these energies quickly converge to a bulk value of around 0.8–0.9 eV in agreement with the studies cited above. The observed differences between configurations located at the same depth can be explained by the small lattice distortions associated with the reconstruction of the surface. The stable configuration closest to the surface is obtained when He is positioned in a tetrahedral site directly below one of the surface dimers. The available volume is there much smaller than in bulk tetrahedral sites, which leads to a much higher formation energy of 1.73 eV and sizeable changes of the surface reconstruction. Because of its high formation

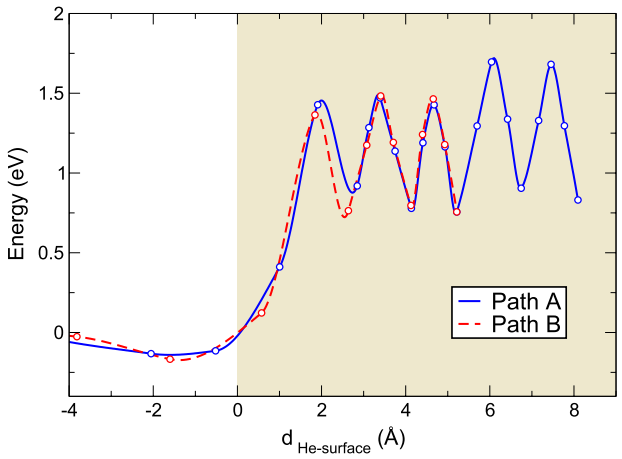

Figure 4. Energy variation for the A (straight blue line) and B (dashed red line) paths as a function of the He position relative to the surface (defined positive for He into the surface). The circles represent the computed NEB points, and the lines are guides for the eyes.

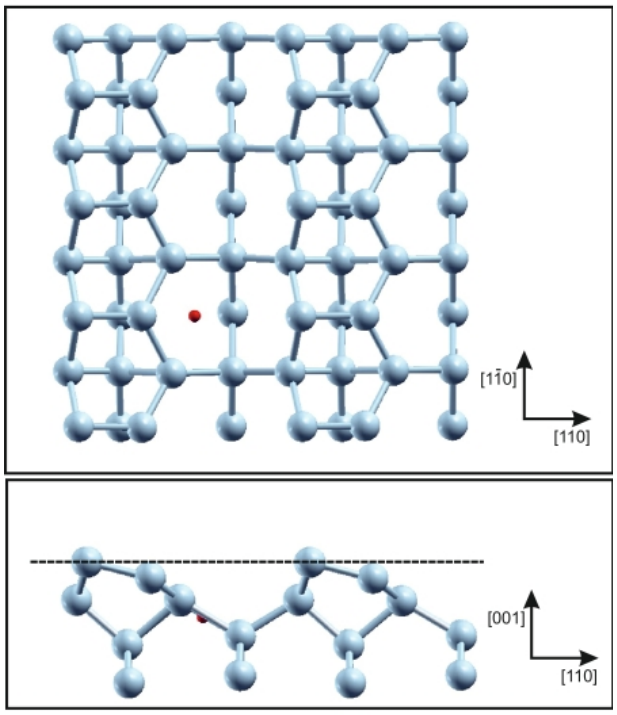

Figure 5. Top and side views of the first saddle configuration along the A path, corresponding to He entering into the Si(001) surface through a pseudo-hexagonal site.

energy this configuration is unlikely to play a role during desorption, and can be safely disregarded.

Based on the examination of the formation energies of the stable configuration, we investigated two possible paths for He diffusion, shown in figure 3. In both paths, the He atom enters the surface from the groove between surface dimer rows. He diffusion directly through a dimer row seems unlikely because of the prohibitive formation energy of the first-encountered stable site. We performed NEB calculations for these two paths, using three optimized replicas for each NEB run between consecutive stable positions. The remaining unknowns were the starting positions when the He is located out of the surface. It was unwise to try to determine the stable He position on the surface since DFT is not appropriate for physisorption. Moreover we assumed that He atoms in bubbles are in a fluid state, i.e. they are characterized by a high mobility and no stationary positions relative to the surface. Then we considered starting configurations where the distance between He and the surface is large enough for their interaction to be negligible, and He is roughly on top of the first stable tetrahedral sites. The energy of these configurations corresponds to the sum of the energies of an isolated He atom and the Si(001) slab. It is used as reference energy for NEB calculations.

Our computed minimum energy paths (MEPs) are shown in figure 4. Since He interstitial diffusion relies on a simple mechanism with the He atom migrating between tetrahedral and hexagonal sites, it is possible to use the distance between the He and the surface (defined at the position of the topmost Si atoms) as the reaction coordinate. Examination of the path A clearly shows that a bulk-like migration is obtained when the He is located deep into the surface, with a migration energy range of 0.8–0.9 eV, in good agreement with previous works [15, 17, 31]. Note that the sudden energy increase occurring approximately 5 Å below the surface is due to the fact that the deepest layers are fixed to bulk positions. The energy maximum of about 1.7 eV corresponds approximately to the sum of formation and migration energies, as depicted in figure 1. Focusing on the vicinity of the surface, it appears that the energy barriers are lower than those deeper in the bulk, for both paths. Of special interest is the first barrier E^s for the He atom to leave the cavity. Here we found energy barriers of 1.43 eV and 1.36 eV for the A and B paths, respectively. Those are reached when the He atom enters the silicon surface from the groove between dimer rows. The two possible saddle configurations correspond to He in pseudo-hexagonal sites, as shown in figure 5. Both are alike hexagonal sites in bulk silicon, except for slight distortions because of surface dimerization. The asymmetry of the reconstruction explains the small differences obtained for the first energy barriers between the A and B paths.

Our computed energies for the first barrier E^s are lower than the sum of the formation and migration energies of the He interstitial, as shown in figure 1. This suggests that a Si(001) surface is not a limiting factor for He desorption from a cavity, i.e. it is more permeable than the bulk. The surface of any He-filled bubble is necessarily characterized by several orientations, among which the (001) kind is always present due to its low energy [29] and geometry requirements. As a result, other orientations do not need to be investigated. In fact, even if other surface orientations would hinder desorption, the helium atom would escape the cavity through the (001) surface. Therefore, our result confirms the general statement that the activation energy for helium desorption is simply given as the sum of the formation energy plus the migration energy of the interstitial He, without taking into account temperature and pressure.

4. Ne:Si(001) system

In a second step, we investigated the case of Ne. Experimentally, Ne desorption from silicon is not observed [8, 9, 14, 23], which suggests that the associated activation energy must be relatively high. This is in agreement with the few available theoretical works. In fact, assuming that the desorption activation energy is given by the sum of the energies for Ne interstitial formation and migration, values of 3.6 eV [17] and 5.6 eV [16] have been computed. Here, we performed a systematic search for stable interstitial configurations for Ne in our system, similarly to what we did for He. All investigated sites were found to be stable, with interstitial formation energies ranging from 2 to 2.3 eV. These values are in good agreement with our earlier calculation of interstitial Ne in bulk silicon [17], the small difference being explained by a much smaller plane wave cutoff and a different k-point sampling here.

Unlike for He, we found that when a Ne atom is initially located in the tetrahedral site directly below a surface dimer, it tends to relax towards the surface. The final configuration is characterized by a breaking of the surface dimer, with the Ne atom between the two Si atoms and at the same height. This geometry is close to a bond-centred structure, which is found to be most stable for neutral atomic hydrogen in silicon [32], but it has never been tried for Ne to the best of our knowledge. The formation energy is 1.49 eV, thus lower than for bulk tetrahedral configurations. It is then a suitable candidate as an intermediate configuration during desorption.

NEB calculations were performed for the same A and B paths as for He, in addition with a new C path starting from the surface configuration discussed above. The energy variations as a function of the Ne atom depth are reported in figure 6. We found a similar behaviour to that for He. Deep into the surface, the migration energy was computed in the range 1.1–1.3 eV, in good agreement with our previous calculation for Ne in bulk Si [17]. Combined with the interstitial formation energy, it gives an activation energy for desorption of about 3.3 eV. Also, it is clear that the first energy barriers encountered by the Ne atom to enter the surface are much lower than this value. In fact, we computed energy barriers of 2.80 eV and 2.54 eV for the A and B paths, respectively. The additional C path requires a much higher energy of 3.36 eV, since the Ne atom has to migrate through the unstable space below surface dimers.

Overall, we found that the energy variations for Ne are very close to those computed for He, with a higher magnitude. This suggests that lattice distortions due to surface reconstruction are essentially responsible. The surface dimerization breaks the paths' symmetry, making some easier and others harder.

5. Temperature and pressure effect

We now investigate the desorption process of helium from silicon, taking into account pressure and temperature. Only the case of He is relevant here, since there is no experimental evidence of Ne desorption from silicon [14], in accordance

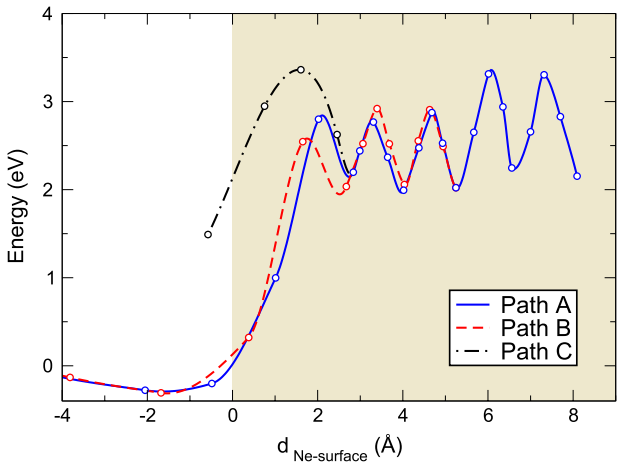

Figure 6. Energy variation for the A (straight blue line), B (dashed red line), and C (dashed-point black line) paths as a function of the Ne position relative to the surface (defined positive for Ne into the surface). The circles represent the computed NEB points, and the lines are guides for the eyes.

with the large energy barriers that we computed. For helium, experiments indicate that the desorption process involves helium atoms contained in well-defined bubbles, which can be observed by transmission electron microscopy. The bubble size depends on the thermal conditions during implantation or post-implantation annealing treatment. However, in most cases and especially in the reported desorption investigations, the cavity diameter ranges from about 10 to 25 nm [12, 22]. Griffioen *et al* [13] measured an activation energy of 1.7 eV for He desorption at a temperature of about 1050 K. More recently, Godey *et al* reported an activation energy of 1.8 eV [6], for a higher temperature of 1150 K. This is in full agreement with another study by Oliviero *et al* who also reported an activation energy of 1.8 eV for a similar temperature [7].

Since we have shown previously that the internal surfaces of bubbles do not act as an additional barrier, the activation energy for desorption ΔE is obtained as the energy difference between two states, He as an interstitial freely migrating in the silicon bulk (diluted state), and He in the cavity (fluid state). The diluted state energy is then the sum of the formation energy of a He interstitial and of its migration energy. Since the hexagonal site is the saddle point for the migration of the He interstitial, this sum is also equal to the formation energy $E_{\mathrm{H}}^{\mathrm{f}}$ of this configuration. In the cavity, in the fluid state, the energy of a single He is the chemical potential μ of the fluid system. Then we have

$$\Delta E = E^{\mathrm{f}} + E^{\mathrm{m}} - \mu = E_{\mathrm{H}}^{\mathrm{f}} - \mu. \qquad (1)$$

For the diluted state, we found a value of 1.7 eV for $E_{\mathrm{H}}^{\mathrm{f}}$ from our first-principles calculations, but at $T = 0$ K. High temperatures are required for helium desorption, for which several additional contributions to the energy have to be taken into account [34]. In the case of point defects, the main contribution has a vibrational origin, and usually reduces the energy required for defect formation. For instance, Al-Mushadani and Needs computed the free energy of a

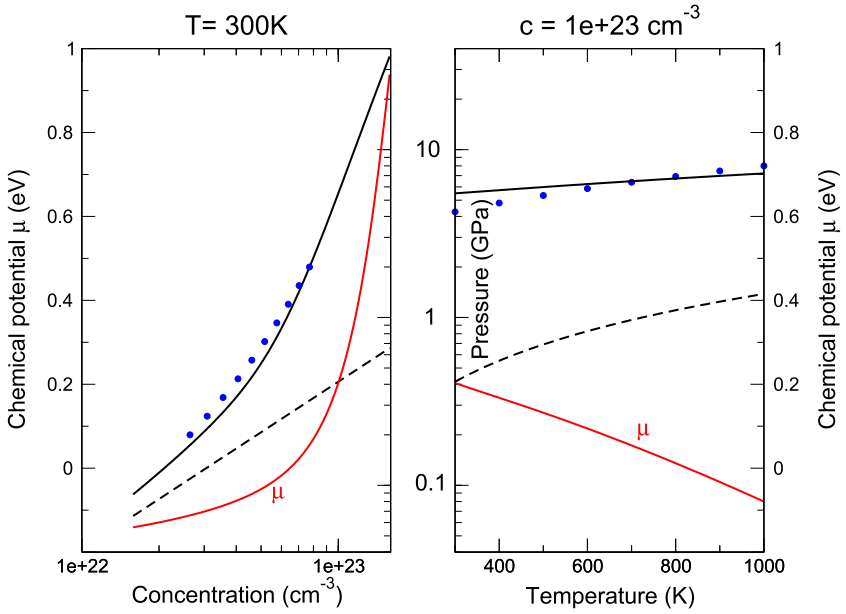

Figure 7. Variations of pressure in GPa (black lines) and chemical potential μ in eV (red lines) as a function of concentration (cm^{-3}) at $T = 300$ K (left), and as a function of temperature (K) at a concentration of 10^{23} cm^{-3} (right), computed with the ultradense fluid model [5]. The dashed lines show the pressure variation obtained with the perfect gas model, and the blue dots are the data calculated from the equation of state of Mills *et al* [33].

silicon interstitial in a hexagonal site and of a vacancy [35]. At 1100 K, they found a 0.4 eV decrease of the formation energy for the former and a 0.9 eV decrease for the latter. The vibrational contributions are larger in the case of a vacancy, since the introduction of a defect leads to a substantial softening of phonons. Although an interstitial introduces additional localized modes, the phonon spectrum is very close to the silicon bulk one, which explains the smaller vibrational energy. Inclusion of the vibrational energy contribution $F(T)$ in our previous expression leads to

$$\Delta E(T,P) = (E_{\mathrm{H}}^{\mathrm{f}})_{T=0} + F(T) - \mu(T,P) \quad (2)$$

$$= 1.7\ \mathrm{eV} + F(T) - \mu(T,P). \quad (3)$$

Unfortunately, no data for $F(T)$ are available for a He interstitial in silicon. Vibrational free energy calculations are feasible at the first-principles accuracy level [36], especially in the framework of the harmonic approximation, but remain a formidable and expensive task that is out of the scope of this work. Here, we estimate the vibrational contribution $F(T)$ by assuming that the He interstitial is equivalent to a quantum harmonic oscillator, which is decoupled from the silicon lattice. This model is likely to be appropriate since the silicon lattice is weakly perturbed by the presence of the He interstitial (deformations of 2–3% only). This approach has already been used by Cerofolini *et al* [5]. The vibrational free energy $F(T)$ is then simply given by [36]

$$F(T) = 3kT \ln\left[\sinh\left(\frac{h\nu}{2kT}\right)\right]. \quad (4)$$

Assuming $\nu = 10^{13}$ s^{-1}, we computed $F(1050\ \mathrm{K}) \simeq -0.4$ eV and $F(1150\ \mathrm{K}) \simeq -0.5$ eV. The agreement with the value of -0.4 eV computed for a Si interstitial in a hexagonal site [35] is reassuring.

We now consider a cavity containing a homogeneous fluid helium to determine $\mu(T,P)$. The system state is characterized by a pressure, a temperature and a concentration, whose dependent variations are described by an equation of state. In our investigations, we used the ultradense fluid model to describe our pressurized helium system [5]. The results of the model are reported in figure 7 for two different states. The computed pressure variations are in excellent agreement with the data derived from high-pressure fluid helium experiments [33]. Conversely, the perfect gas model is clearly not appropriate here due to the high pressure involved. The ultradense fluid model allows one to compute the chemical potential $\mu(T,P)$, i.e. the energy of a single He in our case, as a function of these variables. The main issue here is that while we have a pretty good knowledge of the temperature during desorption experiments, determination of the pressure inside cavities is extremely difficult to achieve. Such a feat has been achieved at room temperature in the case of He-filled cavities in metal [37, 38] and in silicon [39], using spatially resolved electron energy-loss spectroscopy measurements. In the case of silicon, an average helium density of 86 ± 11 He atoms nm^{-3} (concentration 8.6×10^{22} cm^{-3}) was measured, for a bubble diameter of about 18 nm. Within our model, such a density corresponds to an internal pressures of 3 GPa. Unfortunately, these measurements can hardly be made during desorption experiments.

An interesting alternative way is to combine data available from desorption experiments and from our calculations in order to determine the pressure inside cavities. We first focus on the experiments of Godey *et al* [6] and Oliviero *et al* [7], who both measured an activation energy of $\Delta E = 1.8$ eV at about 1150 K. Using equation (3), we found

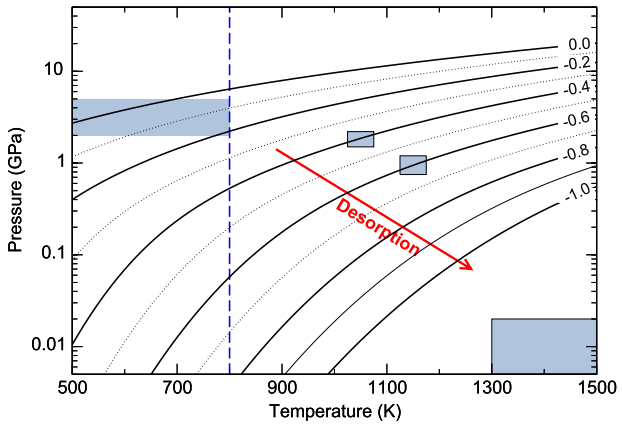

Figure 8. Different (P, T) states of He in bubbles during desorption (blue shaded areas). At temperatures below 800 K, no desorption occurs and the pressure in the bubbles is in the 2–5 GPa range depending on the preparation conditions. At temperatures greater than about 1300 K, very little helium is left in the silicon and there is a very low pressure in the bubbles. At intermediate temperatures, the two small rectangles show the states corresponding to desorption measurements at 1050 K [13] and 1150 K [7]. The lines represent the isoenergy curves for μ (in eV/He atom) as a function of temperature and pressure for helium as computed with the ultradense fluid model [5].

that μ should be equal to -0.6 eV. The isoenergy curves for μ were computed as a function of temperature and pressure and are reported in figure 8. At T= 1150 K, $\mu = -0.6$ eV corresponds to a pressure of about 1 GPa (see figure 8) and a helium concentration of 4×10^{22} cm^{-3}. The earlier experiments of Griffioen *et al* [13] indicate an activation energy of $\Delta E = 1.7$ eV for a maximum of desorption occurring at 1050 K. In that case, the vibrational contribution to the energy is slightly reduced, and we found that μ should now be equal to -0.4 eV. The associated pressure is about 1.8 GPa (figure 8) and the concentration is 6×10^{22} cm^{-3}.

Obviously it is necessary to take into account the effect of temperature on the energy of He in the diluted state. In fact, the assumption that $F(T) = 0$ leads to unrealistically high pressures of 10 GPa inside cavities during desorption experiments. The energy lowering due to vibrational effects in the diluted state partially compensates the decrease of μ in the fluid phase when the temperature is raised. Our investigations indicate that at the desorption maximum in experiments, He-filled bubbles are still highly pressurized, about 1–2 GPa. Although the bubble loses about one half to one third of the He atoms (assuming a realistic initial concentration of 8.6×10^{22} cm^{-3} [39]), the pressure remains substantial due to the high temperatures. Finally, one has to keep in mind that this analysis was made for a single bubble and should be considered an average for a population of bubbles. In fact, complex phenomena like re-capture of He by neighbouring bubbles will certainly occur during desorption experiments, leading to significant disparities between bubbles.

6. Conclusion

Combining density functional theory, the nudged elastic band technique, and the ultradense fluid model, we investigated the desorption process of light noble gas atoms in silicon. In particular, the possible influence of the internal surfaces of bubbles was examined. We found that for a surface with a (001) orientation, the helium atom will migrate through the space between dimer rows. A similar path was obtained for Ne, albeit with a larger migration energy. For the (001) surface, we found that the energy for escaping the bubble is lower than the activation energy required for interstitial diffusion into silicon. Lattice distortion due to surface dimerization is responsible, opening easy paths for gas diffusion. Since facets with (001) orientations or geometrical features of the (001) surface are necessarily present in bubbles, this result indicates that the internal surfaces of bubbles are not a limiting factor during desorption. In view of these results, it would be interesting to investigate non-reconstructed passivated surfaces, such as the dihydride H:Si(001) surface. This surface could possibly behave as an additional barrier for desorption since the low lattice distortion and the expected repulsion between the noble gas and the surface hydrogen atoms are likely to considerably hinder desorption.

Finally, we studied the desorption process in the case of helium considering temperature and pressure, modelling the diluted state (He in silicon) and the fluid state (He in a bubble). We found that vibrational contributions to the energy of the diluted state have to be taken into account in order to compute realistic pressures in the bubbles. Comparing with desorption experiments, we determined that the maximum of desorption corresponds to a bubble pressure of about 1–2 GPa.

Acknowledgments

Marie-Laure David and Erwan Oliviero are gratefully acknowledged for fruitful discussions and for a critical reading of the paper. This work was partly supported by the GNR MATINEX.

References

[1] Donnelly S E 1985 The density and pressure of helium in bubbles in implanted metals: a critical review *Radiat. Effects* **90** 1
[2] DonnellyS E and EvansJ H (ed) 1991 *Fundamental Aspects of Inert Gases in Solids* (New York: Plenum)
[3] Trinkaus H and Singh B N 2003 Helium accumulation in metals during irradiation—where do we stand? *J. Nucl. Mater.* **323** 229
[4] Lucas G and Schäublin R 2009 Stability of helium bubbles in alpha-iron: a molecular dynamics study *J. Nucl. Mater.* **386–388** 360
[5] Cerofolini G F, Corni F, Frabboni S, Nobili C, Ottaviani G and Tonini R 2000 Hydrogen and helium bubbles in silicon *Mater. Sci. Eng. Rep.* **27** 1
[6] Godey S, Ntsoenzok E, Sauvage T, van Veen A, Labohm F, Beaufort M-F and Barbot J-F 2000 Helium desorption from cavities induced by high energy ^{3}He and ^{4}He implantation in silicon *Mater. Sci. Eng.* B **73** 54
[7] Oliviero E, David M-L, Beaufort M-F, Barbot J-F and van Veen A 2002 On the effects of implantation temperature in helium implanted silicon *Appl. Phys. Lett.* **81** 4201

[8] Oliviero E, Peripolli S, Amaral L, Fichtner P F P, Beaufort M F, Barbot J F and Donnelly S E 2006 Damage accumulation in neon implanted silicon *J. Appl. Phys.* **100** 043505
[9] Beaufort M-F, Barbot J-F, Drouet M, Peripolli S, Oliviero E, Amaral L and Fichtner P F P 2007 Nanocavities induced by neon plasma based ion implantation in silicon *Nucl. Instrum. Methods Phys. Res.* B **257** 750
[10] Raineri V, Battaglia A and Rimini E 1995 Gettering of metals by he induced voids in silicon *Nucl. Instrum. Methods Phys. Res.* B **96** 249
[11] Raineri V, Saggio M and Rimini E 2000 Voids in silicon by he implantation: from basic to applications *J. Mater. Res.* **15** 1449
[12] Frabboni S, Corni F, Nobili C, Tonini R and Ottaviani G 2004 Nanovoid formation in helium-implanted single-crystal silicon studied by *in situ* techniques *Phys. Rev.* B **69** 165209
[13] Griffioen C C, Evans J H, De Jong P C and van Veen A 1987 Helium desorption/permeation from bubbles in silicon: a novel method of void production *Nucl. Instrum. Methods Phys. Res.* B **27** 417
[14] van Wieringen A and Warmoltz N 1956 On the permeation of hydrogen and helium in single crystal silicon and germanium at elevated temperatures *Physica* **22** 849
[15] Alatalo M, Puska M J and Nieminem R M 1992 First-principles study of He in Si *Phys. Rev.* B **46** 12806
[16] Estreicher S K, Weber J, Derecskei-Kovacs A and Marynick D S 1997 Noble-gas-related defects in Si and the origin of the 1018 meV photoluminescence line *Phys. Rev.* B **55** 5037
[17] Charaf Eddin A, Lucas G, Beaufort M F and Pizzagalli L 2009 DFT calculation of the stability and mobility of noble gas atoms in silicon *Comput. Mater. Sci.* **44** 1030
[18] Santamarìa-Pérez D, Mukherjee G D, Schwager B and Boehler R 2010 High-pressure melting curve of helium and neon: deviations from corresponding states theory *Phys. Rev.* B **81** 214101
[19] Jónsson H, Mills G and Jacobsen K W 1998 Nudged elastic band method for finding minimum energy paths of transitions *Classical and Quantum Dynamics in Condensed Phase Simulations* ed B J Berne, G Ciccotti and D F Coker (Singapore: World Scientific) chapter 16, p 385
[20] Raineri V, Coffa S, Saggio M, Frisina F and Rimini E 1999 Radiation damage-He interaction in He implanted Si during bubble formation and their evolution in voids *Nucl. Instrum. Methods Phys. Res.* B **147** 292
[21] Fichtner P F P, Kaschny J R, Behar M, Yankov R A, Mücklich A and Skorupa W 1999 The effects of the annealing temperature on the formation of helium-filled structures in silicon *Nucl. Instrum. Methods Phys. Res.* B **148** 329
[22] Beaufort M-F, Oliviero E, Garem H, Godey S, Ntsoenzok E, Blanchard C and Barbot J-F 2000 Defects in silicon induced by high energy helium implantation and their evolution during anneals *Phil. Mag.* B **80** 1975
[23] Oliviero E, Peripolli S, Fichtner P F P and Amaral L 2004 Characterization of neon implantation damage in silicon *Mater. Sci. Eng.* B **112** 111
[24] Hohenberg P and Kohn W 1964 Inhomogeneous electron gas *Phys. Rev.* **136** B864
[25] Kohn W and Sham L J 1965 Self-consistent equations including exchange and correlation effects *Phys. Rev.* **140** A1133
[26] Giannozzi P *et al* 2009 Quantum espresso: a modular and open-source software project for quantum simulations of materials *J. Phys.: Condens. Matter* **21** 395502
[27] Perdew J P, Burke K and Ernzerhof M 1996 Generalized gradient approximation made simple *Phys. Rev. Lett.* **77** 3865
[28] Ramstad A, Brocks G and Kelly P J 1995 Theoretical study of the Si(100) surface reconstruction *Phys. Rev.* B **51** 14504
[29] Stekolnikov A A, Furthmüller J and Bechstedt F 2002 Absolute surface energies of group-IV semiconductors: dependence on orientation and reconstruction *Phys. Rev.* B **65** 115318
[30] Zavodinsky V G, Gnidenko A A, Misiuk A and Bak-Misiuk J 2005 *Ab initio* simulation of high pressure influence on He–H interaction in silicon *Vacuum* **78** 247
[31] Jung P 1994 Diffusion of implanted helium in Si and SiO_2 *Nucl. Instrum. Methods Phys. Res.* B **91** 362
[32] van de Walle C G 1994 Energies of various configurations of hydrogen in silicon *Phys. Rev.* B **49** 4579
[33] Mills R L, Liebenberg D H and Bronson J C 1980 Equation of state and melting properties of ^{4}He from measurements to 20 kbar *Phys. Rev.* B **21** 5137
[34] Estreicher S K and Sanati M 2006 Predicting the energetics of defects at $t > 0$ K *Physica* B **376/377** 940
[35] Al-Mushadani O K and Needs R J 2003 Free-energy calculations of intrinsic point defects in silicon *Phys. Rev.* B **68** 235205
[36] Estreicher S K, Sanati M, West D and Ruymgaart F 2004 Thermodynamics of impurities in semiconductors *Phys. Rev.* B **70** 125209
[37] Taverna D, Kociak M, Stéphan O, Fabre A, Finot E, Décamps B and Colliex C 2008 Probing physical properties of confined fluids within individual nanobubbles *Phys. Rev. Lett.* **100** 035301
[38] Fréchard S, Walls M, Kociak M, Chevalier J P, Henry J and Gorse D 2009 Study by eels of helium bubbles in a martensitic steel *J. Nucl. Mater.* **393** 102
[39] David M-L, Pailloux F, Mauchamp V and Pizzagalli L 2011 *In situ* probing of helium desorption from individual nanobubbles under electron irradiation *Appl. Phys. Lett.* **98** 171903